

# Hemodynamic Monitoring via Sequential Inference for Safety Assurance of Physiological Closed-Loop Controllers: Fluid Resuscitation and Sedation Case Study

## Weidi Yin; Ali Tivay; Jin-Oh Hahn (University of Maryland)

#### Motivation

- ❖ Fluid resuscitation and intravenous (IV) sedation can interfere with each other in a conflicting manner, which can possibly drive a patient to a dangerous physiological state: (i) fluid resuscitation to achieve an arterial blood pressure (BP) target dilutes the sedative drug in the blood and weakens its intended effect; (ii) IV sedation interrupts fluid resuscitation by lowering BP.
- Although closed-loop controlled treatments appear to successfully drive a patient to desired BP and sedation targets, the patient's hemodynamics represented by cardiac output (CO) and total peripheral resistance (TPR) can be driven to an unacceptably dangerous state.
- However, hemodynamic variables such as CO and TPR cannot be readily measured in real-world clinical practice.

## **Research Goal and Novelty**

- ❖ Objective: To demonstrate the potential of model-based sequential inference approach to hemodynamic monitoring in patients receiving fluid resuscitation and IV sedation, using extended Kalman filter (EKF) and unscented Kalman filter (UKF) as illustrative examples.
- Novelty: This work is perhaps the first endeavor to leverage closed-loop state estimation in hemodynamic monitoring problems.

## **Learning Objectives**

- Understand that closed-loop controlled critical care treatments administered to a patient can interfere and conflict with each other, which can drive a patient receiving the treatments to dangerous physiological states.
- Understand that patient safety during closed-loop controlled critical care treatments may only be recognized via hemodynamic monitoring capable of inferring internal hemodynamics state of the patients.
- Understand that mathematical patient models and modern sequential inference methods can be combined to furnish hemodynamic monitoring capabilities required for safe closed-loop controlled critical care treatments.

#### **Mathematical Model**

- Blood volume(BV) kinetics in the arterial and venous circulations.
- Capillary-tissue fluid exchange.
- Autonomic regulation of CO, TPR and unstressed venous BV.
- Sedative pharmacology.

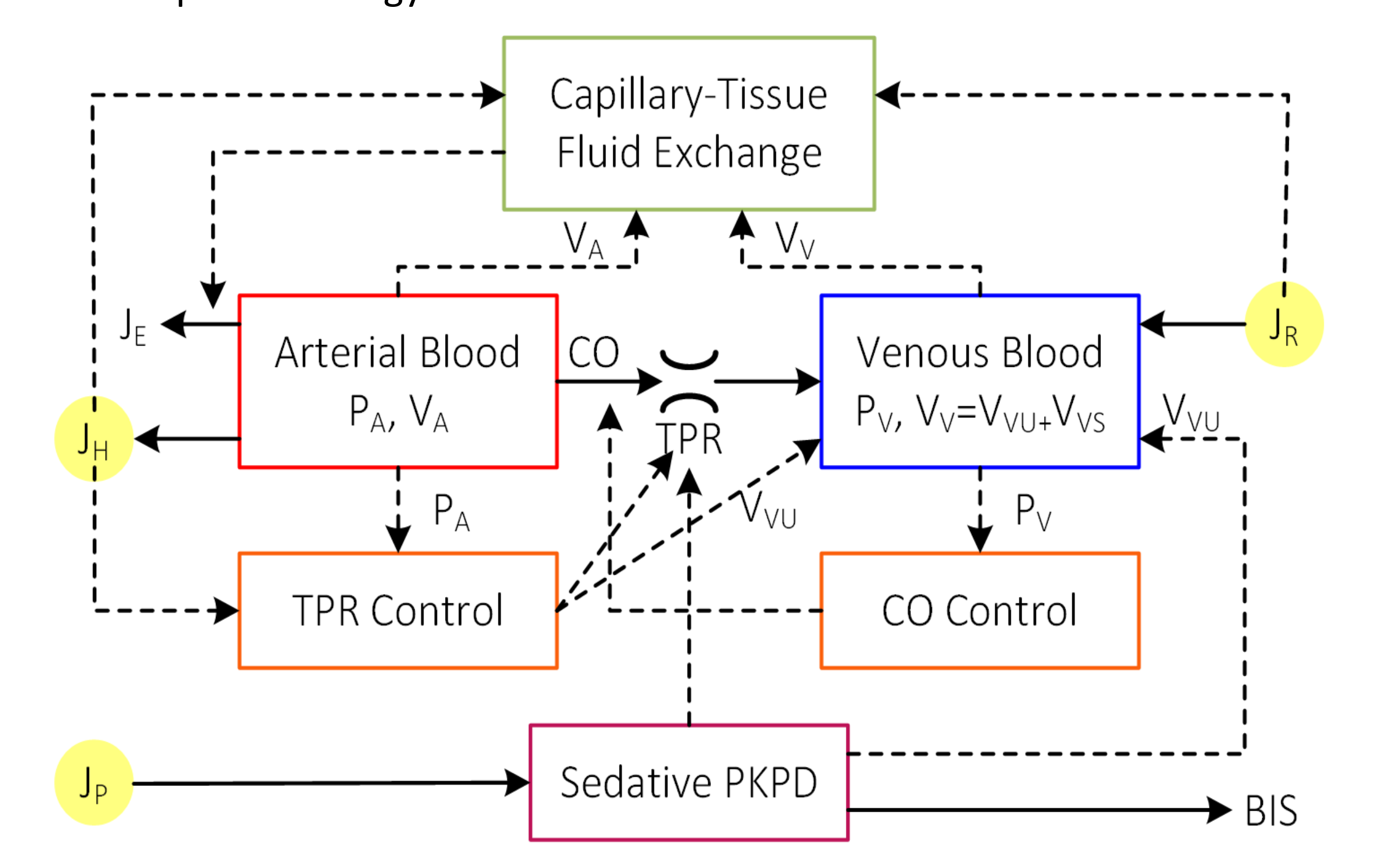


Figure 1. A mathematical model to replicate the combined physiological effects of hemorrhage resuscitation and intravenous (IV) sedation

### Virtual Patient Generation for Design and Evaluation

- Using a collective variational inference (C-VI) method we developed (Figure 2), the virtual patient (VP) generator was derived.
- Estimating the latent parameters from given data reduces to inferring the exact yet intractable posterior density:

$$p(\phi, \theta, n|u, y) = p(\phi, \theta, n, u, y)/p(u, y)$$

Leveraging modern variational inference, we specified an approximate posterior density  $q(\phi, \theta, \mathbf{n} | \mathbf{v})$  and inferred it by minimizing the Kullback-Leibler divergence  $D_{KL}(\mathbf{v})$ :

$$D_{KL}(\mathbf{v}) = \mathbb{E}_{q} [\log q(\phi, \theta, \mathbf{n} | \mathbf{v}) - \log p(\phi, \theta, \mathbf{n} | \mathbf{u}, \mathbf{y})]$$

- ❖ We derived an evidence lower bound and estimated **v** by maximizing:  $L(\mathbf{v}) = \log p(\mathbf{y}) - D_{KL}(\mathbf{v})$ 
  - $= \mathbb{E}_{q}[\log p(\mathbf{y}|\mathbf{\theta}, \mathbf{n}, \mathbf{u}) + \log p(\mathbf{\theta}|\mathbf{\phi}) + \log p(\mathbf{n}) + \log p(\mathbf{\phi}) \log q(\mathbf{\phi}, \mathbf{\theta}, \mathbf{n}|\mathbf{v})]$

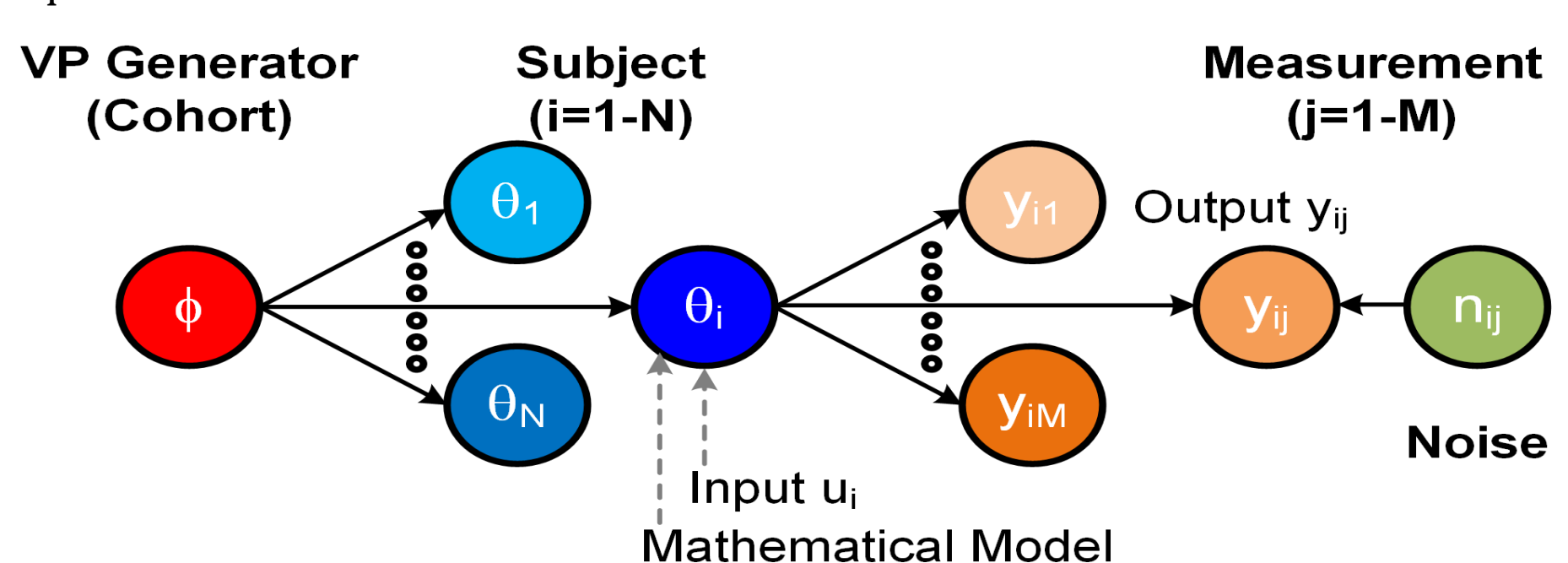


Figure 2. A probabilistic graphical model that structurizes the hierarchical relationship between a cohort and subjects therein into a VP generator.

## **Hemodynamic Monitoring**

☐ Extended Kalman Filter

\*Reformulate the mathematical model into a state space representation:  $\dot{x}(t) = f(x(t), u(t), \theta) + w(t)$ 

$$y(t_k) = \begin{bmatrix} P_A(t_k) \\ BIS(t_k) \end{bmatrix} = h(x(t_k)) + v(t_k)$$

- Noting that the most prominent source of process noise is the parametric uncertainty, we defined w(t) and its covariance matrix as:  $w(t) = J_{\theta}(t)\Delta\theta(t), \qquad Q_{w}(t) = J_{\theta}(t)Q_{\theta}J_{\theta}^{T}(t)$
- Construct the EKF using the most likely model parameters and their covariances associated with the VP generator.
- Derive the most likely CO and TPR estimates and their respective confidence intervals from the state and its covariance estimates.
  - In the prediction step, we solved the state equation and its corresponding covariance equation between the measurement  $\dot{\hat{x}}(t) = f(\hat{x}(t), u(t), \theta)$ time instants:  $\dot{P}(t) = F(t)P(t) + P(t)F^{T}(t) + Q_{w}(t), t_{k-1} \le t \le t_{k}$
  - ❖ In the update step, we corrected the state estimate and its covariance using the sensor measurements:

$$K(t_k) = P^{-}(t_k)H^{T}(t_k)[H(t_k)P^{-}(t_k)H^{T}(t_k) + Q_R]^{-1}$$
 
$$\hat{x}(t_k) = \hat{x}^{-}(t_k) + K(t_k)[y(t_k) - h(\hat{x}(t_k))], \qquad P(t_k) = [I - K(t_k)H(t_k)]P^{-}(t_k)$$
 Unscented Kalman Filter

- Similar to EKF, we defined process noise w(t) and its covariance estimates based on parametric uncertainty.
- In the prediction step, we predicted states and its corresponding covariance using sigma points:

$$\gamma^{i}(t) = f(\chi_{i}), \quad \hat{x}(t) = \sum_{i=0}^{2n} W_{i}^{m} \gamma^{i}(t)$$

$$P(t) = \sum_{i=0}^{2n} W_{i}^{c} (\gamma^{i}(t) - \hat{x}(t)) (\gamma^{i}(t) - \hat{x}(t))^{T} + Q_{w}(t)$$

In the update step, we corrected the state estimate and its covariance using the sensor measurements:

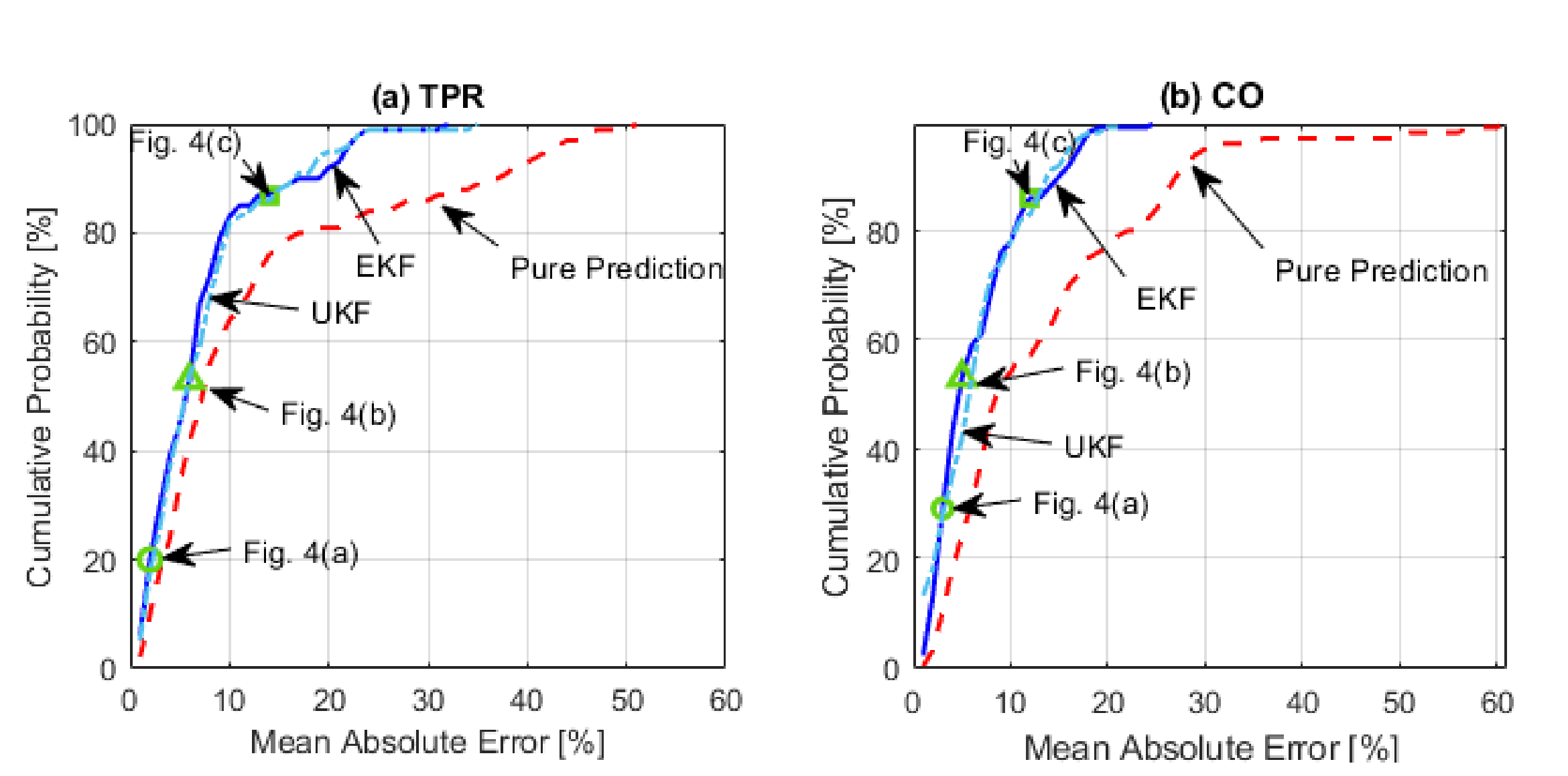
$$\begin{split} \xi^{i}(t_{k}) &= h(\chi_{i}), \ \ \hat{y}(t_{k}) = \sum_{i=0}^{2n} W_{i}^{m} \xi^{i}(t_{k}) \\ P_{yy}(t_{k}) &= \sum_{i=0}^{2n} W_{i}^{c} \left( \xi^{i}(t_{k}) - \hat{y}(t_{k}) \right) \left( \xi^{i}(t_{k}) - \hat{y}(t_{k}) \right)^{T} + Q_{R} \\ P_{xy}(t_{k}) &= \sum_{i=0}^{2n} W_{i}^{c} \left( \gamma^{i}(t_{k}) - \hat{x}(t_{k}) \right) \left( \xi^{i}(t_{k}) - \hat{y}(t_{k}) \right)^{T} \\ \hat{x}(t_{k}) &= \hat{x}^{-}(t_{k}) + K(t_{k})(y(t_{k}) - \hat{y}(t_{k})), \qquad K(t_{k}) = P_{xy}(t_{k})P_{yy}^{-1}(t_{k}) \\ P(t_{k}) &= P^{-}(t_{k}) - K(t_{k})P_{yy}K^{T}(t_{k}) \end{split}$$

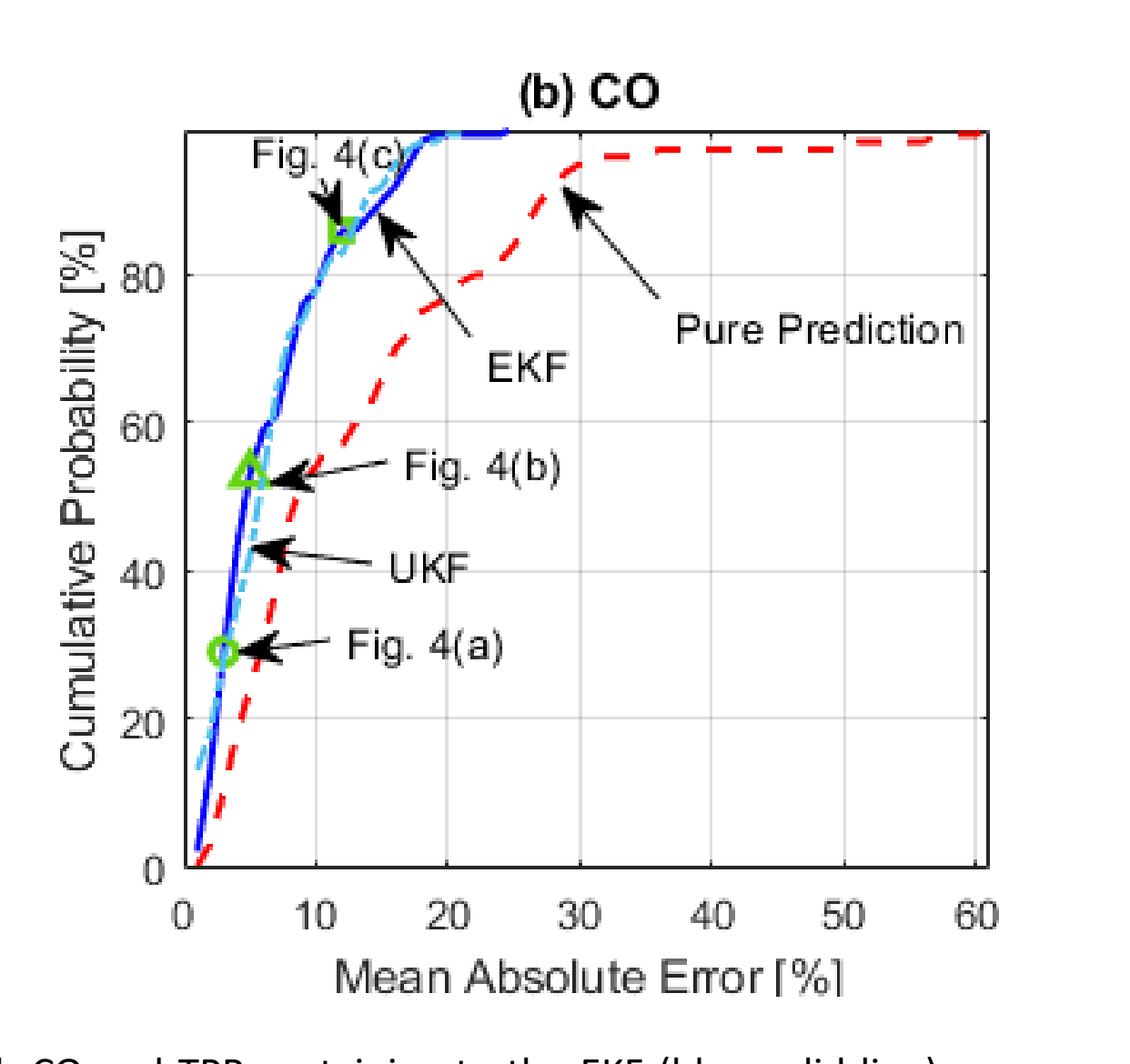
#### **In Silico Evaluation Results**

- The EKF and UKF exhibited significantly superior accuracy to pure prediction in both accuracy and trending ability (Table I).
- The performance of the EKF and UKF were consistent against VP variability: in terms of mean absolute error (MAE), EKF and UKF both had small MAE in most VPs with only a small number of VPs having large MAE (Figure 3).
- \* The EKF and UKF achieved tight tracking of CO and TPR in many VPs (Figure 4).
- \* The EKF and UKF estimated all the state variables with adequate accuracy (Figure 5,6).
- The EKF and UKF both appeared to exhibit CO estimation accuracy and trending ability comparable to the existing AP-based pulse-contour CO(PCCO) monitors.
- \* The limit of agreement(LoA) in CO estimation associated with the EKF was -1.3-1.1 lpm(with UKF was -1.2-1.1 lpm), which was superior to most PCCO monitors reported in recent articles. Besides, the r value associated with EKF(and UKF) based on the CO tracking was higher on the average than the pooled r value associated with the PCCO monitors reported(0.71).
- The EKF(and UKF) based hemodynamic monitoring has unique practical advantages relative to the PCCO monitors: (i) The EKF(and UKF) based monitoring employs only mean AP measurement, while PCCO monitors require the entire AP waveform measurement. (ii) The EKF(and UKF) based monitoring allows for CO and TPR estimation with an explicit account for the IV sedation effect. In contrast, the PCCO monitors are inherently blinded to the influences of sedative

Table 1. . Cardiac output (CO) and total peripheral resistance (TPR) estimation accuracy associated with EKF, UKF and pure prediction. ME: mean error. MAE: mean absolute error. SD: standard deviation. IQR: inter-quartile range. \*: p<0.05 (paired t-test). †: p<0.05 (Wilcoxon rank-sum test)

**Pure Prediction** 0.6 (0.3-0.9) 0.32 (0.15-0.50) -0.2±1.7 0.82±0.04 (7.2% (4.2%-13.6%)) 1.2(0.7-2.3)





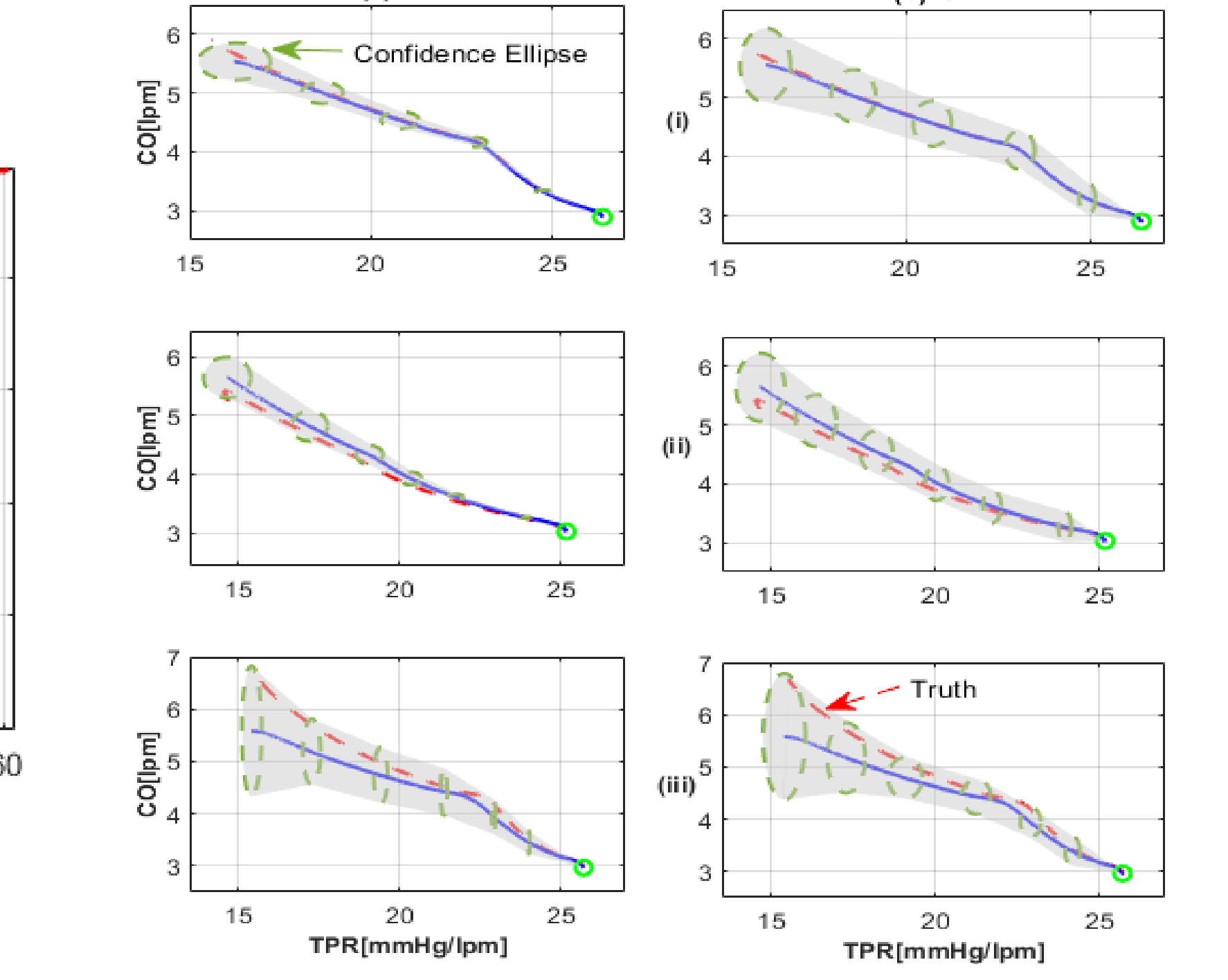
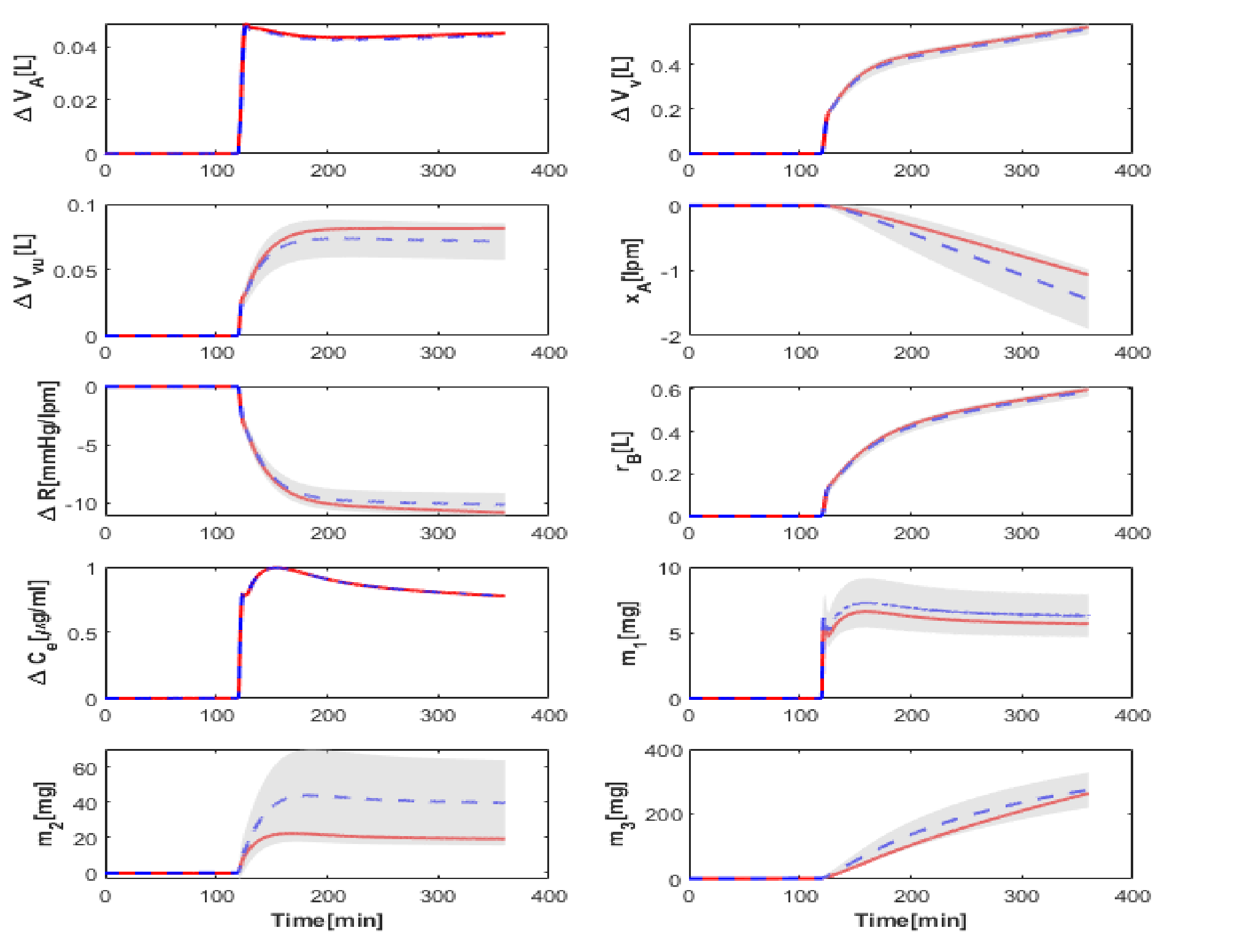


Figure 3. Cumulative distribution of MAE associated with CO and TPR pertaining to the EKF (blue solid line), UKF (light blue dashed-dot line) and open-loop pure prediction (red dashed line).

Figure 4. Representative examples of (i) successful, (ii) typical, and (iii) less successful estimation of CO and TPR based on the (a) EKF and (b) UKF.



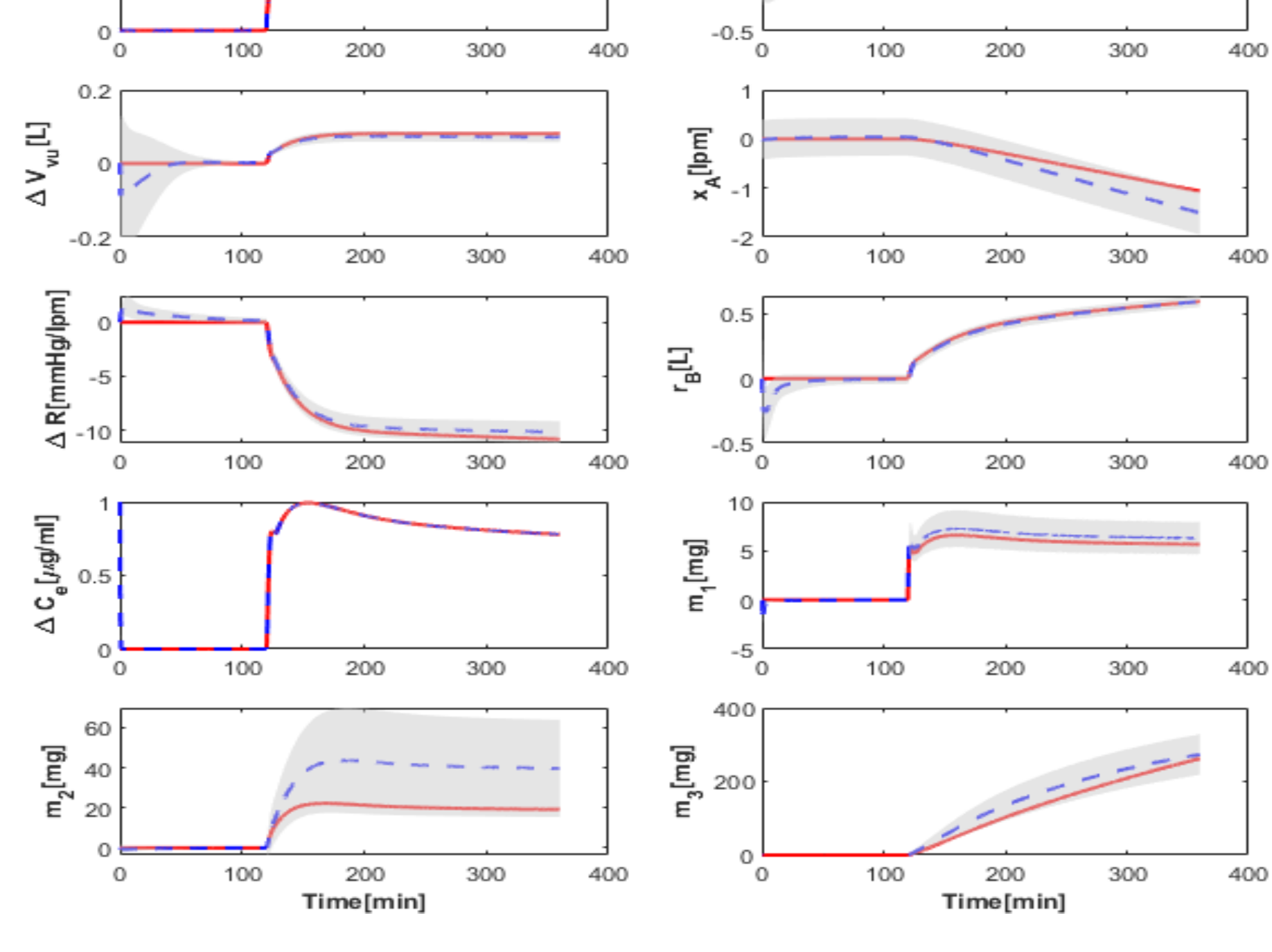


Figure 5. A representative example of true versus EKF-estimated states. These state estimates correspond to Figure 4(a). Red dashed lines: true states. Blue solid lines: EKF-estimated states Grey shades: confidence intervals (±2 standard deviations).

Figure 6. A representative example of true versus UKF-estimated states. These state estimates correspond to Figure 4(a). Red dashed lines: true states. Blue solid lines: UKF-estimated states. Grey shades: confidence intervals (±2 standard deviations).